Electronic Supplementary Material (ESI) for Catalysis Science & Technology.

Supporting Information

Photocatalytic coupled redox cycle for two organic transformations over Pd/carbon nitride composites

*Qiaohui Jia, Sufen Zhang, Xiaoxia Jia, Xiaoyang Dong, Ziwei Gao, and Quan Gu**

Key Laboratory of Applied Surface and Colloid Chemistry, Ministry of Education, School of Chemistry and Chemical Engineering, Shaanxi Normal University, Xi'an, 710062, China.

*E-mail: guquan@snnu.edu.cn

1. Experimental section

1.1 Materials

Melamine (99%), bromobenzene (99%), 4-bromoethylbenzene (99%), 1-bromo-4-(tert-butyl)benzene (97%), 1-bromo-4-fluorobenzene (98%), 1-bromo-4-chlorobenzene (99%), 4-iodotoluene (99%), 4-chlorotoluene (99%), benzyl alcohol (99%), 1-phenylethanol (98%), 2-phenylethanol (99.5%), 3-phenyl-1-propanol (99%), 4-methylbenzyl alcohol (98%), 4-methoxybenzyl alcohol (98%), methyl 4-(hydroxymethyl)benzoate (97%), 4-chlorobenzyl alcohol (99%), and 2-heptanol (98%) were purchased from Aladdin. 4-bromotoluene (99%+), 4-bromobenzonitrile (99%), 1-bromo-4-methoxybenzene (99%), *p*-benzoquinone (99%), and diisopropylethylamine(99%) were purchased from Adamas Reagent, Ltd. Potassium tetrachloropalladate (99%), Palladium diacetate (99%), and 1-bromo-4-nitrobenzene (98%) were acquired from energy chemical. 2-bromotoluene (99%), and 3-bromotoluene (99%) were obtained from 3A Chemicals. Anhydrous lithium chloride (AR), potassium chloride (AR), anhydrous ethanol (AR), anhydrous potassium carbonate (99%) were obtained from Guangzhou Jinhuada Chemical Reagent Co., Ltd. Sodium borohydride (AR) and ethylene glycol (AR) was purchased from Sinopharm Chemical Reagent Co. Ltd. All chemicals were used without further purification.

1.2 Preparation of graphitic carbon nitride (g-C_3N_4)

g-C_3N_4 powder was prepared by thermal polycondensation of melamine. Typically, 3 g of melamine was put in a crucible with cover and annealed at 550 ^oC for 4 h with a heating rate of 5 ^oC min^{-1} under an air atmosphere in a muffle furnace. The obtained yellow product was g-C_3N_4 powder.

1.3 Preparation of $Pd_{2.0}$/g-C_3N_4

The synthesis of $Pd_{2.0}$/g-C_3N_4 containing 2% Pd was the same as the preparation of Pd/CN-T. 10 mL K_2PdCl_4 aqueous solution (2.454 mg/mL) was added in g-C_3N_4 suspension (400 mg g-C_3N_4 powder in 10 mL water) under vigorous stirring for 3 h in a 100 mL beaker. Thereafter, the powder product was collected via centrifugation, washed with distilled water, ethanol, and acetone, respectively, and dried in a vacuum oven at 40 ^oC overnight. The obtained Pd modified g-C_3N_4 powder was re-dispersed in 40 mL water under vigorous stirring in a 100 mL beaker and reduced by $NaBH_4$ (10 ml, 0.5 M) followed by centrifugation, washing and drying.

1.4 Synthesis of Pd nanoparticles

3 mg of palladium diacetate were dispersed in 5 mL ethylene glycol and the mixture was then sonicated for 90 min at room temperature in a bath sonicator. The final product was separated and washed with ethanol three times by centrifugation (10,000 rpm, 20 min).

1.5 Characterization

The X-Ray Diffraction (XRD) patterns of all samples were collected on Rigaku D/Max2550VB+/PC (Cu Kα source) at a scan rate of 2.4^{o} min^{-1}. Scanning Electron Microscopy (SEM) images were obtained on a HITACHI SU8220 microscope at an acceleration voltage of 5 kV. Transmission Electron Microscopy (TEM) images and element mapping were obtained by a Tecnai G2 F20 transmission electron microscopy (FEI, USA) at an accelerating voltage of 200 kV. Fourier Transform Infrared (FTIR) spectra were derived from Perkin Elmer Fourier transform infrared spectrometer GX. Photoelectron Spectroscopy (XPS) spectra were determined on a VG ESCALAB 250 XPS system with a monochromatized Al Kα X-ray source (15 kV, 200 W). Nitrogen adsorption-desorption isotherms were performed at 77 K using Micromeritics ASAP 2010 equipment. The Electron Paramagnetic Resonance (EPR) spectroscopy was carried out via a Bruker A-300-EPR X-band spectrometer. Raman spectra were measured by Renishaw In Via Reflex Micro Raman Spectrometer with an excitation wavelength of 325 nm. Solid-state ^{13}C Nuclear Magnetic Resonance (NMR) spectroscopy was performed on a Bruker Advance DRX500 spectrometer. UV/vis Diffuse Reflectance spectrum (UV/Vis DRS) was measured by a UV/vis spectrophotometer (UV-Lambda 950, Perkin Elmer). Photoluminescence (PL) spectra were accomplished in solid with Shimadzu RF5301 Spectrofluorophotometer with an excitation wavelength of 380 nm. Time-Resolved Photoluminescence (TRPL) decay measurements were carried out on a time-correlated single photon counting (TCSPC) Edinburgh FLS 920 fluorescence spectrometer. The photoelectrochemical tests were carried out by using the conventional three-electrode electrochemical cell including a working electrode, a platinum wire counter electrode, and an Ag/AgCl reference electrode. The prepared photoelectrodes were used as the working electrode and irradiated under visible light in Na_2SO_4 solution (0.5 M).

2. Supplementary Figures and Tables

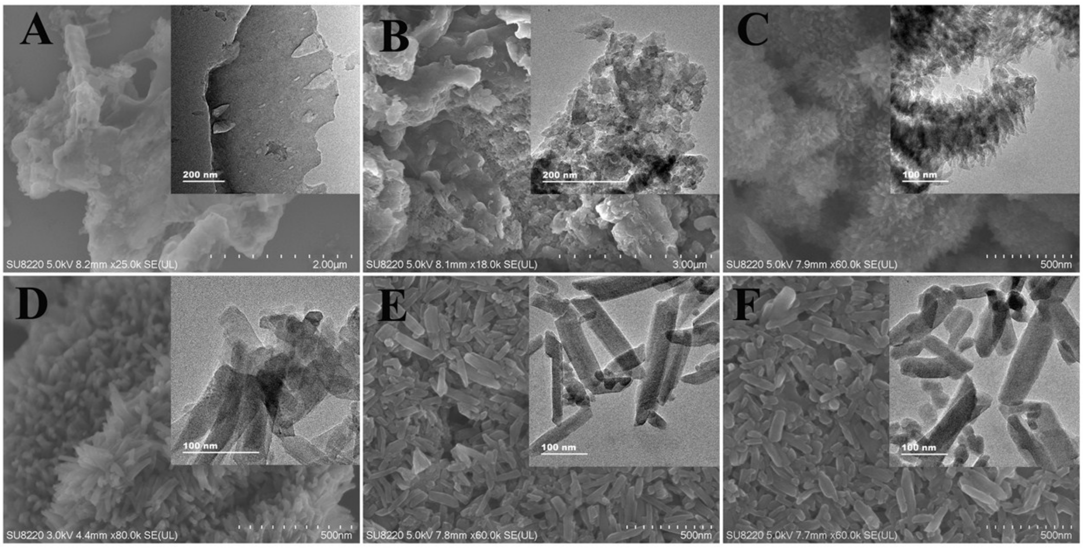

Fig. S1 SEM and TEM images of pristine g-C_3N_4 (A), CN-300 (B), CN-400 (C), CN-450 (D), CN-500 (E), and CN-550 (F).

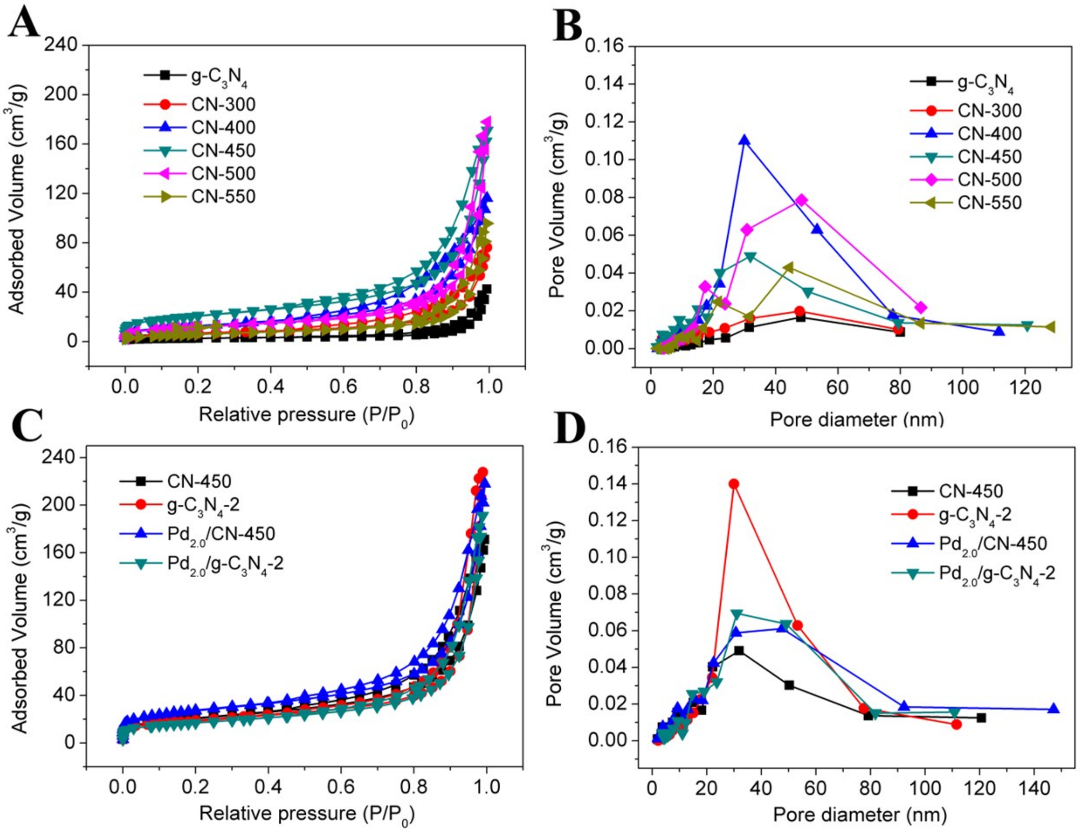

Fig. S2 the nitrogen adsorption-desorption isotherms (A and C) and the corresponding pore-size distribution curves (B and D) of samples.

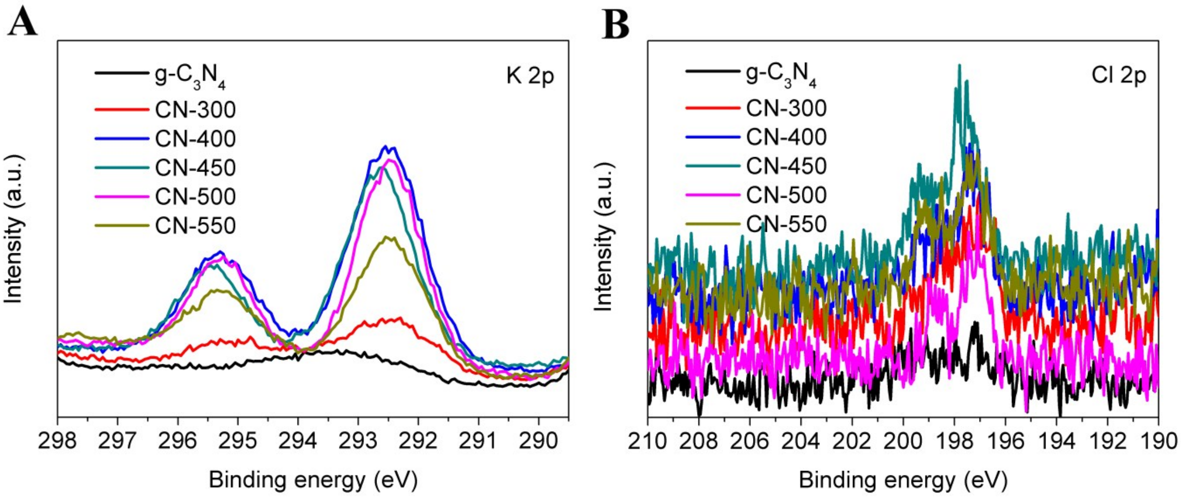

Fig. S3 the high-resolution K 2p and Cl 2p XPS spectra of pristine g-C_3N_4 and CN-T obtained by the post-annealing of g-C_3N_4 in molten salts (T=300, 400, 450, 500, and 550, refers to the post-annealing temperature).

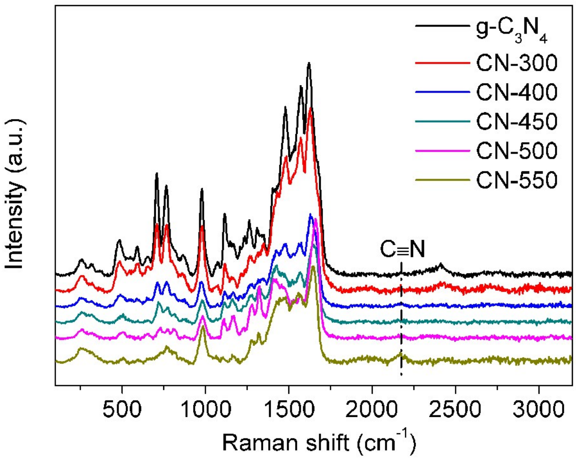

Fig. S4 Raman spectra of pristine g-C_3N_4 and CN-T.

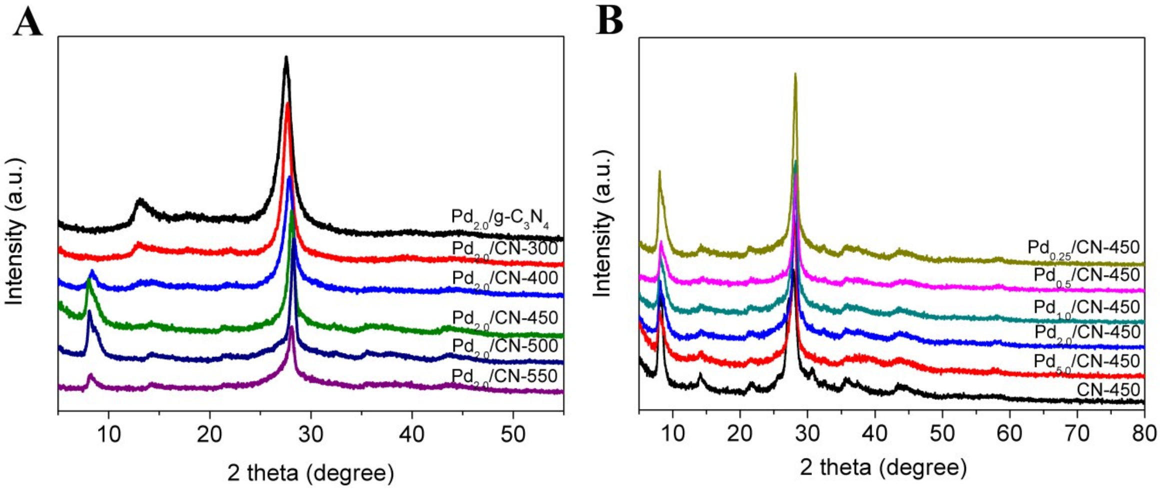

Fig. S5 (A) XRD patterns of $Pd_{2.0}/g\text{-}C_3N_4$ and $Pd_{2.0}$/CN-T; (B) XRD patterns of Pd_x/CN-450 with different Pd loading amount.

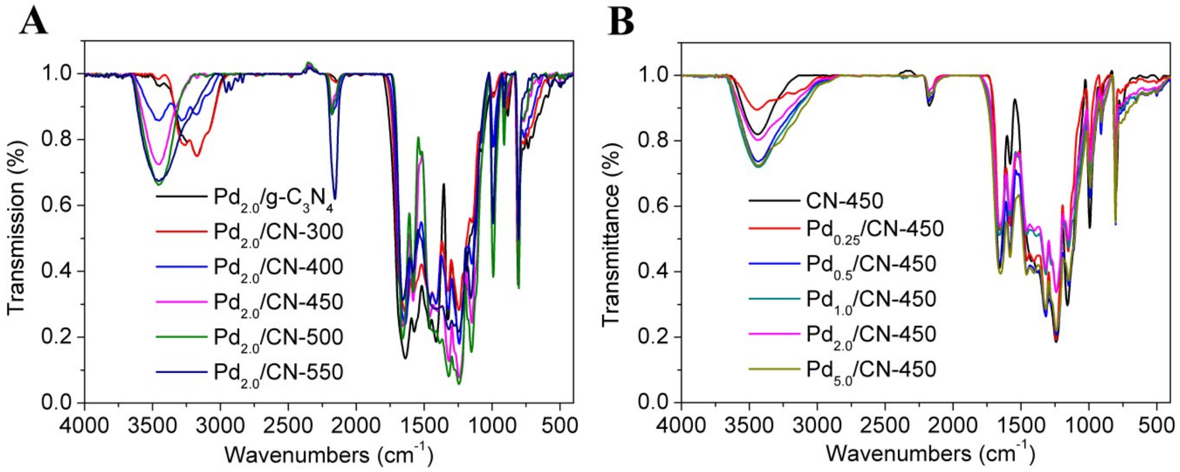

Fig. S6 (A) FTIR spectra of $Pd_{2.0}/g\text{-}C_3N_4$ and $Pd_{2.0}$/CN-T; (B) FTIR spectra of Pd_x/CN-450 with different Pd loading amount.

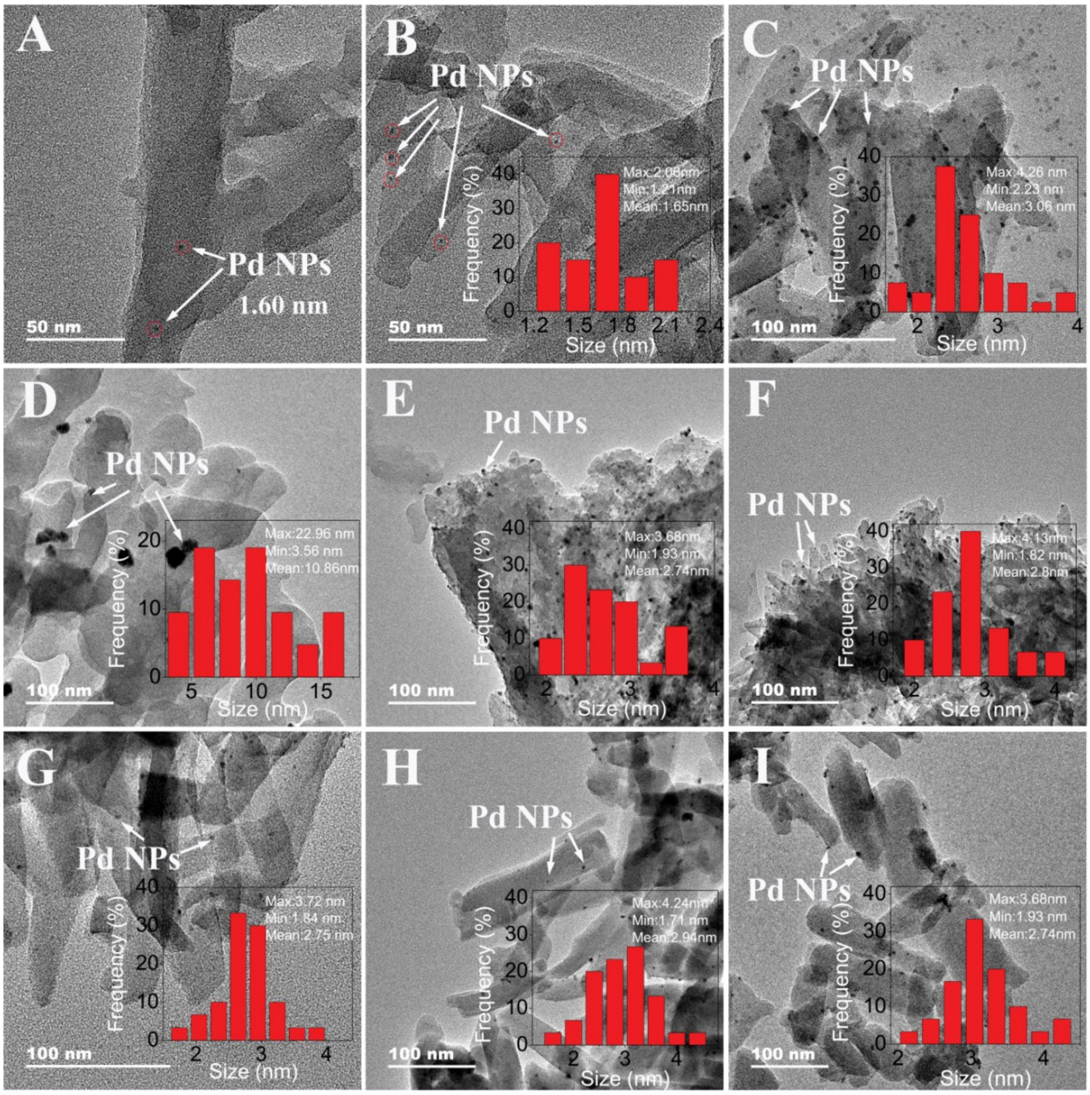

Fig. S7 TEM images of (A) $Pd_{0.5}$/CN-450, (B) $Pd_{1.0}$/CN-450, (C) $Pd_{5.0}$/CN-450, (D) $Pd_{2.0}$/g-C_3N_4, (E) $Pd_{2.0}$/CN-300, (F) $Pd_{2.0}$/CN-400, (G) $Pd_{2.0}$/CN-450, (H) $Pd_{2.0}$/CN-500, and (I) $Pd_{2.0}$/CN-550. Inserts show the statistical size distribution of Pd NPs.

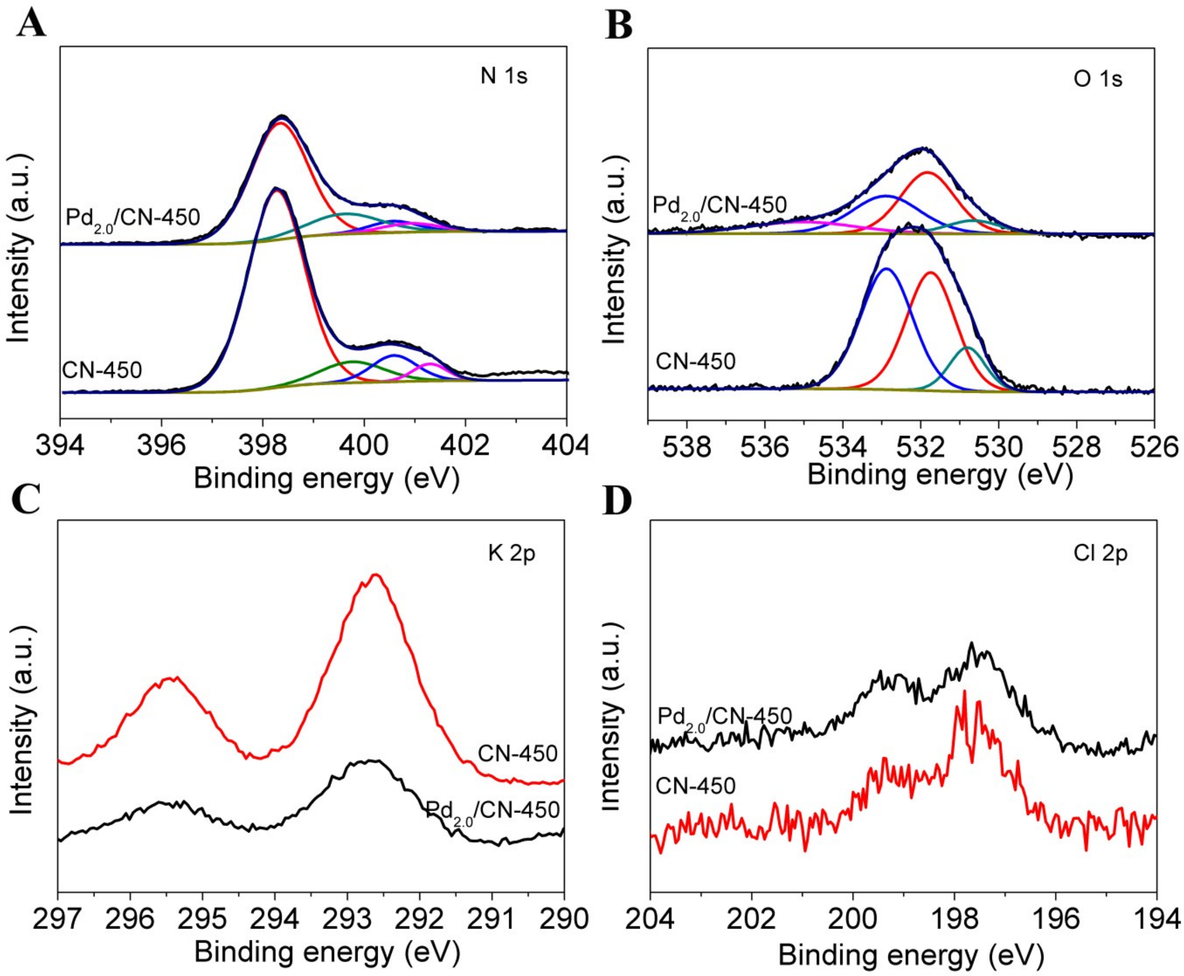

Fig. S8 high-resolution N 1s, O1s, K 2p, and Cl 2p XPS spectra of CN-450 and $Pd_{2.0}$/CN-450.

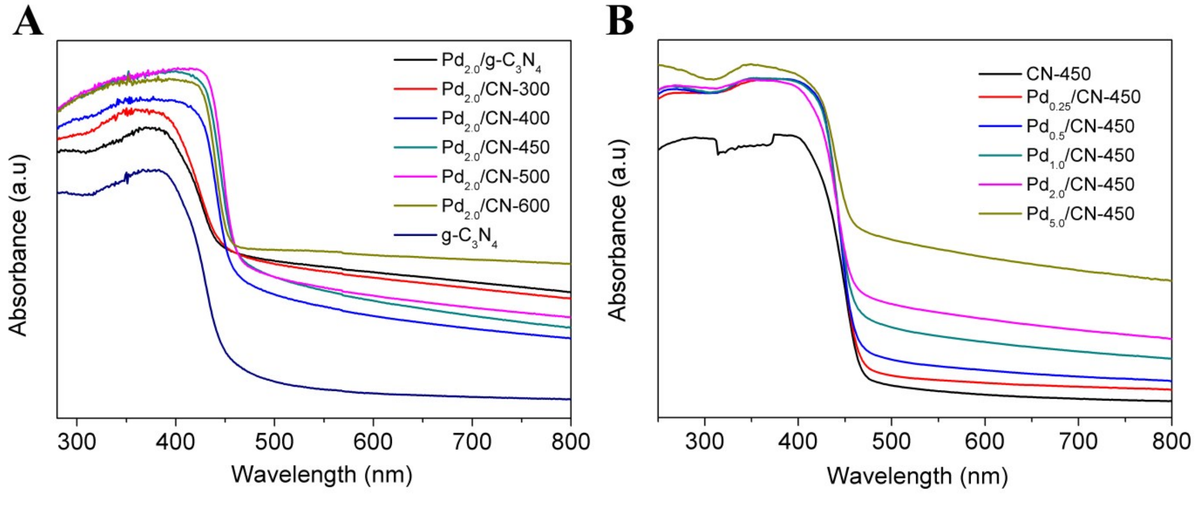

Fig. S9 UV-vis DRS spectra of g-C_3N_4, $Pd_{2.0}$/g-C_3N_4, and $Pd_{2.0}$/CN-T; (B) UV-vis DRS spectra of Pd_x/CN-450 with different Pd loading amount.

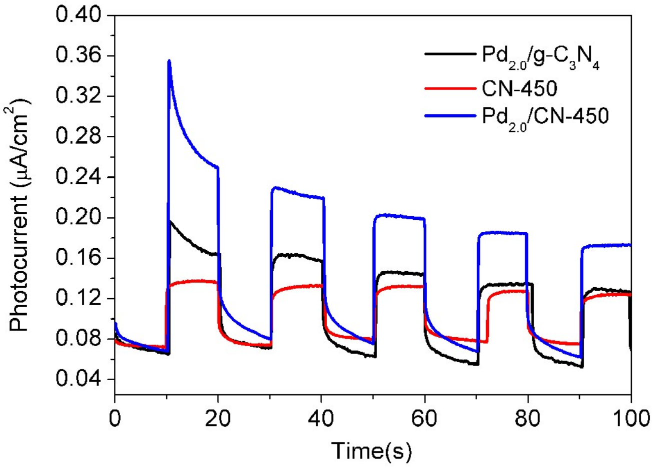

Fig. S10 Photocurrents under visible light irradiation of CN-450, $Pd_{2.0}/g-C_3N_4$, and $Pd_{2.0}$/CN-450.

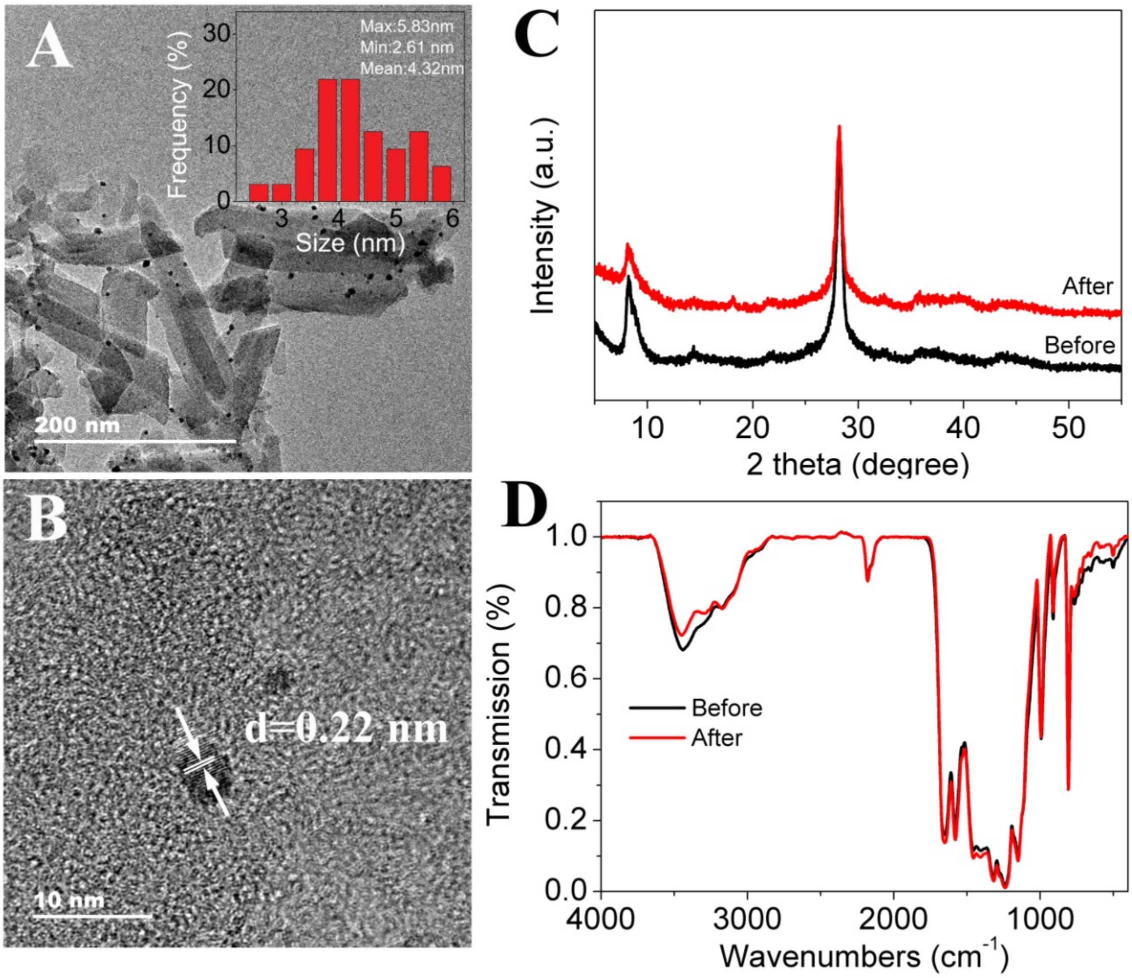

Fig. S11 TEM (A) and HRTME (B) images of $Pd_{2.0}$/CN-450 after the photocatalytic coupled reaction. XRD patterns (C) and FTIR spectra (D) of $Pd_{2.0}$/CN-450 before and after the photocatalytic coupled reaction.

Table S1 BET surface area, pore volume, and pore size of as-prepared samples.

Sample	Pore volume (ml/g)	Pore size (nm)	S_{BET} (m^2/g)
g-C_3N_4 [a]	0.0580	22.48	9.5
g-C_3N_4-2[b]	0.3536	20.14	65.1
CN-300	0.1093	13.64	24.5
CN-400	0.1809	12.89	46.4
CN-450	0.2670	13.44	74.0
CN-500	0.2573	24.01	42.2
CN-550	0.1484	23.75	22.1
$Pd_{2.0}$/CN-450	0.3405	14.64	96.2
$Pd_{2.0}$/g-C_3N_4-2[c]	0.2935	20.31	60.0

[a] g-C_3N_4 was prepared by thermal polycondensation of melamine at 550 °C. [b] g-C_3N_4-2 was prepared by thermal etching of g-C_3N_4 at 520 °C. [c] $Pd_{2.0}$/g-C_3N_4-2 was prepared by loading Pd nanoparticles on g-C_3N_4-2.

Table S2 Element contents of C, N, H, and O in pristine g-C_3N_4, CN-300, CN-400, CN-450, CN-400, and CN-500 determined by elemental analysis.

Sample	Elemental content (wt%)				N/C mole ratio	O/C mole ratio	O/N mole ratio
	N	C	H	O			
g-C_3N_4	56.53	34.03	1.85	4.89	1.425	0.108	0.076
CN-300	54.54	32.94	1.73	8.22	1.418	0.187	0.132
CN-400	50.38	30.24	1.85	10.97	1.429	0.272	0.191
CN-450	44.62	27.34	2.07	16.59	1.399	0.455	0.325
CN-500	41.96	25.95	1.84	16.83	1.385	0.486	0.351
CN-550	40.57	25.26	1.80	17.77	1.377	0.528	0.383

Table S3 Assignments of the FTIR bands of pristine g-C_3N_4, CN-300, CN-400, CN-450, CN-400, and CN-500.

g-C_3N_4	CN-300	CN-400	CN-450	CN-500	CN-550	
FTIR bands/wavenumbers (cm^{-1})						Assignment
-	-	3450	3450	3450	3450	the stretching vibrations of hydroxyl
3171, 3262	3171, 3262	3171, 3262	3171, 3262	3262	-	the stretching vibrations of primary amines or hydrogen-bonding primary amines
3087	3087	3087	-	-	-	the stretching vibrations of secondary amines
-	2167	2167	2167	2167	2167	the vibration of cyano terminal groups
1640, 1569	1640, 1569	1641, 1569	1660, 1579	1660, 1579	1660, 1579	the stretching vibrations of the C=N in C-N heterocycles skeletal
1463, 1413	1463, 1413	1463, 1413	1428	1428	1428	the stretching vibrations of C-N in C-N heterocycles skeletal
-	-	-	1385	1385	1385	the vibrations of C-OH
1324, 1241	1324, 1241	1324, 1241	1324, 1241	1324, 1241	1324, 1241	the stretching vibrations the C-NH-C unit
-	1145	1150	1152	1152	1152	the vibrations of C-O-C v_{as}(C-O-C),
-	990	990	990	990	990	the stretching of N-O groups
807	807	807	807	807	807	the breathing vibrations of heptazine units

Table S4 O/C, NH_x/N, and CN/N mole ratios of pristine g-C_3N_4, CN-300, CN-400, CN-450, CN-400, and CN-500 determined by XPS.

samples	O/C mole ratio	NH_x/N mole ratio	CN/N mole ratio
g-C_3N_4	0.111	0.093	0
CN-300	0.337	0.065	0.006
CN-400	0.382	0.059	0.041
CN-450	0.426	0.056	0.062
CN-500	0.517	0.047	0.068
CN-550	0.933	0.040	0.070

Table S5 XPS peak positions of C1s, N1s, O 1s, K $2p_{3/2}$ and Cl $2p_{3/2}$ of pristine g-C_3N_4, CN-300, CN-400, CN-450, CN-400, and CN-500.

Sample	XPS peak	Peak position (eV)	
g-C_3N_4	C 1s	284.6	contaminant aromatic carbon
		286.1	carbon linked to amino function (C-NH_x, x=1, 2)
		287.8	sp^2-hybridized carbon in tri-s-triazine ring
	N 1s	398.3	sp^2-hybridized nitrogen in tri-s-triazine rings (C-N=C)
		399.6	tertiary nitrogen N-$(C)_3$ groups
		400.8	amino functions caring hydrogen (-NH_x, x=1, 2)
	O 1s	530-534	adsorbed oxygen species on g-C_3N_4
CN-300	C 1s	284.6	contaminant aromatic carbon
		286.2	carbon linked to amino function (C-NH_x, x=1, 2), C-O-C, and C-OH
		287.7	sp^2-hybridized carbon in tri-s-triazine ring
	N 1s	398.3	sp^2-hybridized nitrogen in tri-s-triazine rings (C-N=C)

		399.6	tertiary nitrogen N-(C)$_3$ groups
		400.2	terminal cyano groups
		400.7	amino functions caring hydrogen (-NH$_x$, x=1, 2)
	O 1s	530.5	C=O
		531.8	C-O-C
		532.9	C-OH groups
	K 2p$_{3/2}$	197.4	K$^+$
	Cl 2p$_{3/2}$	292.5	ionic Cl
CN-400	C 1s	284.6	contaminant aromatic carbon
		286.2	carbon linked to amino function (C-NH$_x$, x=1, 2), C-O-C, and C-OH
		287.7	sp^2-hybridized carbon in tri-s-triazine ring
	N 1s	398.2	sp^2-hybridized nitrogen in tri-s-triazine rings (C-N=C)
		399.5	tertiary nitrogen N-(C)$_3$ groups
		400.3	terminal cyano groups
		400.7	amino functions caring hydrogen (-NH$_x$, x=1, 2)
	O 1s	530.5	C=O
		531.7	C-O-C
		532.8	C-OH groups
	K 2p$_{3/2}$	197.4	K$^+$
	Cl 2p$_{3/2}$	292.5	ionic Cl
CN-450	C 1s	284.6	contaminant aromatic carbon
		286.2	carbon linked to amino function (C-NH$_x$, x=1, 2), C-O-C, and C-OH
		287.8	sp^2-hybridized carbon in tri-s-triazine ring
		288.7	C=O groups

	N 1s	398.2	sp^2-hybridized nitrogen in tri-s-triazine rings (C-N=C)
		399.7	tertiary nitrogen N-$(C)_3$ groups
		400.5	terminal cyano groups
		401.0	amino functions caring hydrogen (-NH_x, x=1, 2)
	O 1s	530.7	C=O
		531.7	C-O-C
		532.8	C-OH groups
	K $2p_{3/2}$	197.4	K^+
	Cl $2p_{3/2}$	292.5	ionic Cl
CN-500	C 1s	284.6	contaminant aromatic carbon
		286.3	carbon linked to amino function (C-NH_x, x=1, 2), C-O-C, and C-OH
		287.5	sp^2-hybridized carbon in tri-s-triazine ring
		288.6	C=O groups
	N 1s	398.0	sp^2-hybridized nitrogen in tri-s-triazine rings (C-N=C)
		399.6	tertiary nitrogen N-$(C)_3$ groups
		400.3	terminal cyano groups
		400.9	amino functions caring hydrogen (-NH_x, x=1, 2)
	O 1s	530.5	C=O
		531.7	C-O-C
		532.9	C-OH groups
	K $2p_{3/2}$	197.4	K^+
	Cl $2p_{3/2}$	292.5	ionic Cl
CN-550	C 1s	284.6	contaminant aromatic carbon
		286.1	carbon linked to amino function (C-NH_x,

		x=1, 2), C-O-C, and C-OH
	287.8	sp^2-hybridized carbon in tri-s-triazine ring
	288.7	C=O groups
N 1s	398.0	sp^2-hybridized nitrogen in tri-s-triazine rings (C-N=C)
	399.6	tertiary nitrogen $N-(C)_3$ groups
	400.3	terminal cyano groups
	400.9	amino functions caring hydrogen ($-NH_x$, x=1, 2)
O 1s	530.6	C=O
	531.8	C-O-C
	533.0	C-OH groups
K $2p_{3/2}$	197.4	K^+
Cl $2p_{3/2}$	292.5	ionic Cl

The time-resolved photoluminescence (TRPL) analysis was carried out to investigate the lifetime of photogenerated charge carriers in $g-C_3N_4$, CN-450, $Pd_{2.0}/g-C_3N_4$, and $Pd_{2.0}$/CN-450 samples, as shown in Figure 5C. A tri-exponential fitting was performed for the luminescence decay curves by using the following equation:

$$y = A + B_1 exp(\frac{-t}{\tau_1}) + B_2 exp(\frac{-t}{\tau_2}) + B_3 exp(\frac{-t}{\tau_3})$$

where A is the baseline correction (y-offset), B_1, B_2, and B_3 are pre-exponential factors, and τ_1, τ_2, and τ_3 are the three decay time constants: the radiative process (τ_1), non-radiative process (τ_2), and energy transfer process (τ_3). The mean lifetimes (τ_m) are calculated using the following equation:

$$\tau_m = \frac{\sum_{i=1}^{n} B_i \tau_i^2}{\sum_{i=1}^{n} B_i \tau_i}$$

The decay time constants, the corresponding pre-exponential factors, and the mean lifetime for all the samples are listed in Table S6.

Table S6 The kinetics of emission decay parameters of g-C_3N_4, CN-450, $Pd_{2.0}$/g-C_3N_4, and $Pd_{2.0}$/CN-450 samples.

Sample	τ_1 (ns) (Rel.%)	τ_2 (ns) (Rel.%)	τ_3 (ns) (Rel.%)	τ_m (ns)	Ex (nm)	Em (nm)
g-C_3N_4	1.743 (21.9)	5.155 (56.1)	18.96 (22.0)	7.45	370	450
$Pd_{2.0}$/g-C_3N_4	1.060 (38.7)	3.847 (46.43)	20.88 (14.87)	5.5	370	460
CN-450	1.890 (41.4)	5.503 (42.1)	17.71 (16.5)	5.71	370	440
$Pd_{2.0}$/CN-450	0.877 (40.55)	3.327 (43.76)	17.60 (15.69)	4.58	370	455